CO_2 Photoreduction

Deutsche Ausgabe: DOI: 10.1002/ange.201602796
Internationale Ausgabe: DOI: 10.1002/anie.201602796

A Long-Lived Mononuclear Cyclopentadienyl Ruthenium Complex Grafted onto Anatase TiO_2 for Efficient CO_2 Photoreduction

*Haowei Huang[+], Jinjin Lin[+], Gangbei Zhu, Yuxiang Weng, Xuxu Wang, Xianzhi Fu, and Jinlin Long**

Abstract: *This work shows a novel artificial donor–catalyst–acceptor triad photosystem based on a mononuclear C_5H_5-RuH complex oxo-bridged TiO_2 hybrid for efficient CO_2 photoreduction. An impressive quantum efficiency of 0.56 % for CH_4 under visible-light irradiation was achieved over the triad photocatalyst, in which TiO_2 and C_5H_5-RuH serve as the electron collector and CO_2-reduction site and the photon-harvester and water-oxidation site, respectively. The fast electron injection from the excited Ru^{2+} cation to TiO_2 in ca. 0.5 ps and the slow backward charge recombination in half-life of ca. 9.8 μs result in a long-lived D^+–C–A^- charge-separated state responsible for the solar-fuel production.*

Chemical conversion of carbon dioxide (CO_2) into low-carbon fuels, such as methane (CH_4) and methanol (CH_3OH), at high efficiency and high product selectivity is an ideal solution to global warming and shortages of fossil fuels and carbon resources.[1] One way to accomplish the conversion is through applying artificial photosystems including solar photovoltaic (PV) devices, photoelectrochemical (PEC) cells, and photocatalysis (PC) with electrons and protons derived from water.[2] State-of-the-art PV and PEC systems for the conversion generally yield an efficiency as low as 0.1 % under visible-light irradiation but are believed to be a promising means of addressing the CO_2 conversion issues.[3] Photocatalysis, which involves light-irradiated catalysts including solid catalysts and molecular catalysts, is the simplest CO_2 conversion approach, more amenable to cheap, large-scale applications of low-carbon fuel production.[4] Unluckily, despite intense effort over the last decade, the solar-fuel production by the photocatalyzed conversion of CO_2 and water still faces several challenging issues: 1) The majority of semiconductor photocatalysts, such as TiO_2, ZnO, Zn_2GaO_4, Zn_2GeO_4, ZnS, ZrO_2, $BaTiO_3$, $SrTiO_3$, Ga_2O_3, Zn_2SnO_4, only utilize the UV light region of solar electromagnetic spectrum; 2) currently reported photocatalysts that can work for the conversion in the visible-light region give a low quantum efficiency (QE) of less than 0.1 %;[3,4] 3) the overall eight-electron reduction of CO_2 to low-carbon fuels encounters the competing backward reactions, leading to a heterogeneous product distribution from CO and HCOOH to CH_3OH and CH_4, finally to C_2-hydrocarbons; and 4) understanding of the photocatalyzed CO_2 conversion mechanism still is in its infancy owing to both the complex multielectron-transfer processes and the multi-avenues to final products.

It was well established that the overall conversion of CO_2 and H_2O into CH_4 is made of two electrochemical half-reactions [Eq. (1),(2)].[3]

$$2\,H_2O \rightarrow O_2 + 4\,H^+ + 4\,e^-,\ E^\circ = +0.82\ V \text{ at pH } 7.0 \quad (1)$$

$$CO_2 + 8\,H^+ + 8\,e^- \rightarrow CH_4 + 2\,H_2O,\ E^\circ = -0.24\ V \text{ at pH } 7.0 \quad (2)$$

It requires a high Gibbs free energy at room temperature and standard pressure, but the concerted eight-electron reduction process for CH_4 evolution is kinetically more favorable than the two, four, or six-electron processes corresponding for the production of CO, HCOOH, HCHO, and CH_3OH, which need a more negative electrochemical potential (−0.38 V for CH_3OH, −0.48 V for HCHO, −0.53 V for CO, and −0.61 V for HCOOH).[3] The kinetic considerations mean that the challenge lies mainly in the congregation of eight electrons and reactive substrates at an active center, which performs the eventual formation of C–H bonds.

Inspired by natural photosystems composed of donor–photosensitizer–acceptor (DPA) triads, herein, an artificial donor–catalyst–acceptor (DCA) triad photosystem based on a novel C_5H_5-RuH complex bound to anatase (C_5H_5-RuH-O-TiO_2) hybrid was proposed to perform the CO_2 reduction. Such a molecular hybrid material with the feature of the mononuclear C_5H_5-RuH complex coordinated to three Ti-O sites can function as a visible-light photocatalyst fulfilling the above electrochemical requirements. Ruthenocene was used because it has an oxidation potential (+1.14 V vs. normal hydrogen electrode (NHE)) higher than the water oxidation potential (+0.82 V) and high reactivity to surface acidic hydroxyls of metallic oxides and zeolites.[5] Anatase TiO_2 nanoparticles with rich surface active sites were chosen as the electron collector to carry out the CO_2 reduction. The resultant hybrid just spans the range of the reduction and oxidation potentials relevant to the photocatalyzed reaction, and should move in principle the two half-reactions (Equations (1) and (2)) towards the right, driven by visible light.

[*] H. Huang,[+] J. Lin,[+] Prof. X. Wang, Prof. X. Fu, Prof. J. Long
State Key Laboratory of Photocatalysis on Energy and Environment
College of Chemistry
Fuzhou University
Fuzhou, 350116 (P.R. China)
E-mail: jllong@fzu.edu.cn
Dr. G. Zhu, Prof. Y. Weng
Beijing National Laboratory for Condensed Matter Physics and CAS Key Laboratory of Soft Matter Physics, Institute of Physics, Chinese Academy of Science
No. 8, 3rd South Street, Zhongguancun, Haidian District, Beijing 100190 (P.R. China)
[+] These authors contributed equally to this work.
Supporting information and the ORCID identification number(s) for the author(s) of this article can be found under http://dx.doi.org/10.1002/anie.201602796.

Surprisingly, an unexpected quantum efficiency (QE) of 0.56% is achieved over the optimal hybrid photocatalyst $C_5H_5Ru_{0.6}/TiO_2$ for the CO_2-to-CH_4 conversion under 420 nm light irradiation. The surface CpRuH-O-Ti ($Cp = \eta$-C_5H_5) complex is locally excited by visible light to fast inject electrons into the TiO_2 host in approximately 0.5 ps, forming a long-lived D^+–C–A^+ charge-separated state with a half-lifetime up to 9.8 μs to implement the multiple-electron reduction of CO_2 to CH_4 by H_2O at almost 100% selectivity.

The preparation of the surface C_5H_5-RuH complex proceeds by the chemical grafting of ruthenocene ($(C_5H_5)_2Ru$) on dehydrated anatase TiO_2 surface, that is, Cp_2Ru physically adsorbed on anatase TiO_2 reacts with the isolated hydroxyls to remove a Cp group in a CpH way at 423 K. The remnant C_5H_5-Ru fragment is chemically bonded to surface hydroxyl sites of TiO_2 nanoparticles via the Ti-O-Ru linkage. FTIR spectra (Figure 1 A) clearly display several characteristic IR bands at 1524, 1445, and 1412 cm^{-1} corresponding to the C_5H_5 ligand of the surface Ru complex, indicating that the chemical grafting of Cp_2Ru to anatase TiO_2 nanoparticles is basically in coincidence with those of Cp_2Ni and Cp_2Fe reported in our previous work.[5b,c] The different point is the occurrence of two weak IR bands at 2071 and 2002 cm^{-1} belonging to the stretching vibration of Ru–H bonds.[6] The exposure to air leads to a blue shift from 2002 to 1954 cm^{-1} ($\Delta = 48$ cm^{-1}) and almost disappearance of the 2071 cm^{-1} band due to the coverage of adsorbed H_2O molecules with a characteristic IR band at 1626 cm^{-1}.[7] Importantly, no any changes are discernible on the IR spectra obtained after the exposure for 1 h and 6 months (Supporting Information, Figure S1), indicating that the surface Ru complex is chemically stable for oxygen and wetness, even under an inert atmosphere below 423 K as shown in TPD patterns (Figure S2). All of structural characterizations including XRD, TEM, HRTEM, EDS, and elemental mapping analysis (Figure S4–6) results clearly indicate that the grafted Ru complex is homogeneously dispersed on TiO_2 surface. It does not alter the crystal structure and morphologic characteristics of the parent TiO_2, but modulates its electronic structure and surface properties, as shown by the XPS spectra (Figure S3B,C). The Ru3d XPS peak at approximately 280.4 eV (Figure S3A) demonstrates that the grafted Ru species is still present in +2 oxidation state,[8] whereas the 1s binding energy of the oxygen atoms in $CpRu_x/TiO_2$ shifts from 529.8 to 529.9 eV, and the Ti $2p_{3/2}$ binding energy shifts by 0.2 eV towards low energy. It indicates the electron-donating effect of the grafted Ru complex.

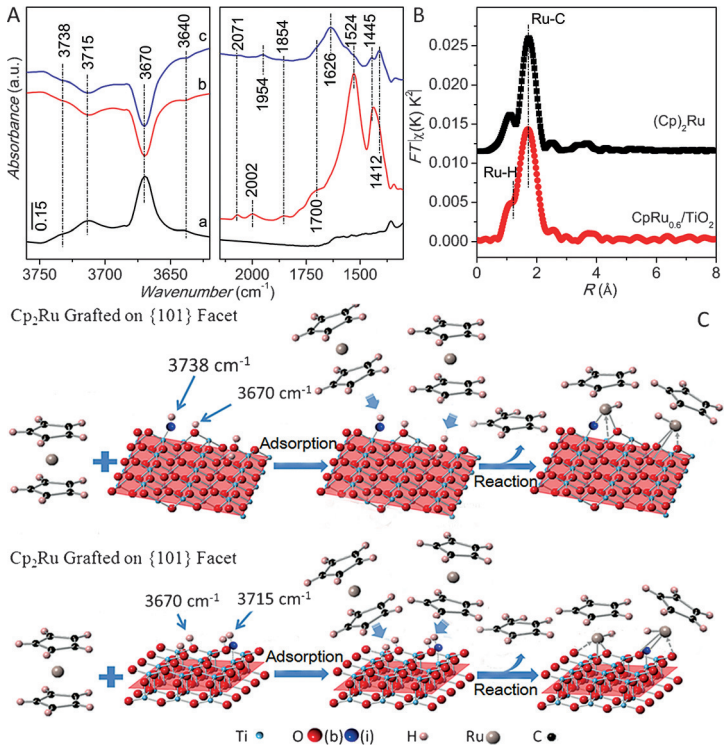

Figure 1. A) IR spectra of TiO_2 before and after grafting reaction with Cp_2Ru: a) TiO_2 dehydrated in vacuum at 673 K for 2 h, where four IR bands belonging to surface hydroxy groups situated at {101} and {001} facets occur at 3738, 3715, 3670, and 3640 cm^{-1}.[5b] b) after reaction at 423 K for 24 h and elimination of the physically adsorbed species at room temperature in vacuum for 2 h; c) after exposure to air, the band at 1524 cm^{-1} has decreased in intensity owing to the adsorption of H_2O molecules on the TiO_2 surface, as illuminated by occurrence of the 1626 cm^{-1} band in (A). B) EXAFS spectra of Cp_2Ru and $CpRu_{0.6}/TiO_2$. C) The chemically grafting of Cp_2Ru on {101} and {001} facets of anatase TiO_2 nanoparticles. (b) and (i) indicate different of oxygen atoms of TiO_2.

The Ru K-edge κ^2-weighted EXAFS spectrum of $CpRu_{0.6}/TiO_2$ (Figure 1 B) gives only a strong oscillation peak, like the reference Cp_2Ru. No Ru–Ru back-scatterings are discernible, indicating that the grafted Ru species are atomically isolated on the TiO_2 surface. The fit results (Table S1, Figure S8) show that each Ru atom in the grafted sample is coordinated on average to three oxygen atoms of TiO_2 lattice with a Ru–O distance of 2.05 Å, to five C atoms with a Ru–C distance of 2.21 Å, and to one H atom with a Ru–H distance of 1.59 Å. The XAFS result thus strongly evidences the formation of a well-defined mononuclear $(\equiv Ti\text{-}O\text{-})_3$ $RuH\text{-}C_5H_5$ surface complex by a pathway proposed in Figure 1 C. The tripodal surface Ru complex is oxo-bridged to the {101} and {001} facets of TiO_2 nanoparticles. Interestingly, the grafted Ru complex results in a wide visible absorption from 400 to 800 nm (Figure S9A), compared to the bare TiO_2 that gives the band-edge absorption at about 380 nm. It can be seen from their difference spectra (Figure S9B) that a main absorption centered at around 414 nm with a long tail occurs in the whole visible region, which was also discerned in the previous work on the Ti-O-M molecular linkages (M = Ni, Mn, Ce).[5b,9] The absorption at 414 nm is attributed to the metal-to-metal charge transfer (MMCT) of a new molecule bonding, Ti-O-Ru. It has nothing to do with the C_5H_5 ligand, as indicated by the uniform UV/Vis DRS spectrum of the $Ru_{0.6}/TiO_2/H_2$ sample prepared by removing the C_5H_5 group of $CpRu_{0.6}/TiO_2$ with H_2 at 573 K for 24 h. These results conclusively indicate that the surface C_5H_5-RuH complex can harvest visible photons by the local surface excitation of Ti^{IV}-O-$Ru^{II} \rightarrow Ti^{III}$-O-$Ru^{III}$.

The CO_2-to-CH_4 conversion is used to evaluate the photocatalytic properties of as-synthesized $CpRu_x/TiO_2$ hybrids. No CH_4 is detected when put the $CpRu_x/TiO_2$ catalysts in a mixture steam of CO_2 and H_2O in dark for 4 h, while visible light ($\lambda > 420$ nm) irradiation of the $CpRu_x/TiO_2$ powders leads to the evolution of CH_4 at room temperature (Figure 2 and Table S3). Its yield steadily

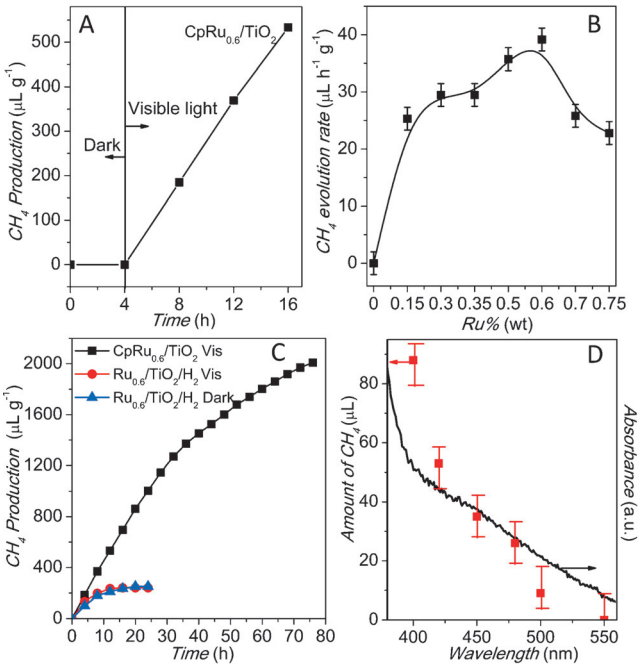

Figure 2. A) CH_4 production of per gram of $CpRu_{0.6}/TiO_2$ under dark and visible-light irradiation. B) The CH_4 revolution rate functions as the grafted amount of Ru. C) The CH_4 production over per gram $CpRu_{0.6}/TiO_2$ and $Ru_{0.6}/TiO_2/H_2$ under visible-light and the $Ru_{0.6}/TiO_2/H_2$ under dark as functions of time. D) Wavelength-dependence of CH_4 production over the $CpRu_{0.6}/TiO_2$ catalyst.

increases with irradiation time (Figure 2 A). Bare TiO_2 does not show CH_4 evolution under visible light irradiation due to no visible light absorption. These results indicate that the conversion is driven by visible light absorption. Moreover, no CH_4 is produced in this photoreaction system without adding CO_2 or/and H_2O, proving that the product CH_4 is really derived from two reactive substrates, CO_2 and H_2O, instead of the C_5H_5 ligand of the grafted surface species. The two isotope-labeling experiment (^{18}O and ^{13}C) results provide the most solid evidence for the electrons of CO_2 photoreduction coming from the water oxidation (Figure S10). The CH_4 evolution rate increases with the Ru grafting and reaches a maximum (44.0 $\mu L\,g^{-1}\,h^{-1}$) at 0.6 wt % Ru content, followed by a considerable decrease (Figure 2 B). The maximal rate of CH_4 evolution is far larger than that (6.0 $\mu L\,g^{-1}\,h^{-1}$) of the reference counterpart prepared by covalent bonding of ligands of $Ru(phen)_2(PIBH)$ (phen = phenanthroline, PIBH = pyridyl benzimidazole hybrid) to surface of anatase TiO_2, and the optimal rate of CH_4 evolution can be enhanced to ca. 80 $\mu L\,g^{-1}\,h^{-1}$ under solar irradiation. The 7-fold enhanced efficiency of CH_4 production originates from the formation of interfacial Ti^{IV}-O-Ru^{II} bonding, which facilities the transfer of photo-generated electrons from the Ru moieties to TiO_2.

Removal of the C_5H_5 organic ligand deactivates the catalyst. The control sample, $Ru_{0.6}/TiO_2/H_2$, gives a low CH_4 production of approximately 240 $\mu L\,g^{-1}$ without visible-light excitation (Figure 2 C), but subjects to quick deactivation, implying that it is a catalytic process, more likely a chemical reaction. Also, another control sample, $Ru_{0.6}/TiO_2/O_2$ prepared by removing the C_5H_5 group of $CpRu_{0.6}/TiO_2$ with O_2 at 673 K for 12 h, is catalytically and photocatalytically inert for the conversion (Table S3). XPS and EXAFS characterizations (Figure S11 and S12) illuminate that the Ru^{II} species are oxidized to +4 oxidation state and present as RuO_2 nanoclusters.[10] These results conclusively indicate that the C_5H_5 organic group bonded to Ru^{II} cation is indispensable for the photocatalyzed CO_2 conversion. Figure 2 D presents the wavelength dependence of CH_4 evolution on the catalyst. The CH_4 production matches well with the diffuse reflectance spectrum of surface Ru complex, confirming that the reaction is indeed induced by light absorption.

Femtosecond time-resolved IR absorption spectroscopy was first used to trace the dynamics of metal-to-metal charge transfer (MMCT) into the surface C_5H_5-RuH-O-Ti complex under 800 nm light irradiation. These structureless broadband spectra in the range of 5000–9000 nm are characteristic of free electrons, and thus this absorbance can be assigned to the intra-band transition from the bottom of conduction band to the upper levels.[11] For the bare TiO_2, it has a band gap energy of around 3.2 eV and no photo-response for visible and near IR light, whereas two-photon absorption occurs with 800 nm excitation,[12] leading to the generation of mobile holes and electrons. As shown in Figure 3 A, it presents the transient absorption with the signal intensity of 0.0035 OD at delay time 1 ps. The absorption unambiguously originates from the photogenerated electrons trapped in conduction band or mid-gap states.[11b,13] The absorption intensity exponentially decreases to approximately 0.0001 OD at delay time 100 ps. For the $CpRu_{0.6}/TiO_2$ (Figure 3 B), the identical absorption as bare TiO_2 means that the trapped electrons are placed in the same environment. No any vibration peaks appear in the observed transient IR spectra except for the interference from those of water molecule. A four-fold enhanced absorbance appears, compared to the bare TiO_2. The transient absorption intensity reaches 0.016 OD at delay time 1 ps and yet decays to 0.004 OD at delay time 100 ps. It implies that the concentration of photo-generated carriers on the excited $CpRu_{0.6}/TiO_2$ sample is four times than that of the bare TiO_2. The increased carrier population can be originated from the MMCT of surface C_5H_5-RuH-O-Ti complex.

Figure 3 C displays the electron decay kinetics of $CpRu_{0.6}/TiO_2$ and bare TiO_2 at 8500 nm. The rising phases of both the kinetics were fitted by convolution of an instrumental response function (0.2 ps in full width at half maximum (FWHM)) with an exponential rising equation corresponding to the electron injection time. The electron injection time for bare TiO_2 by two-photon excitation is 0.3 ps, while the electron injection from C_5H_5 complex to the conduction band of TiO_2 is 0.5 ps (Figure S13). Meanwhile, both of the

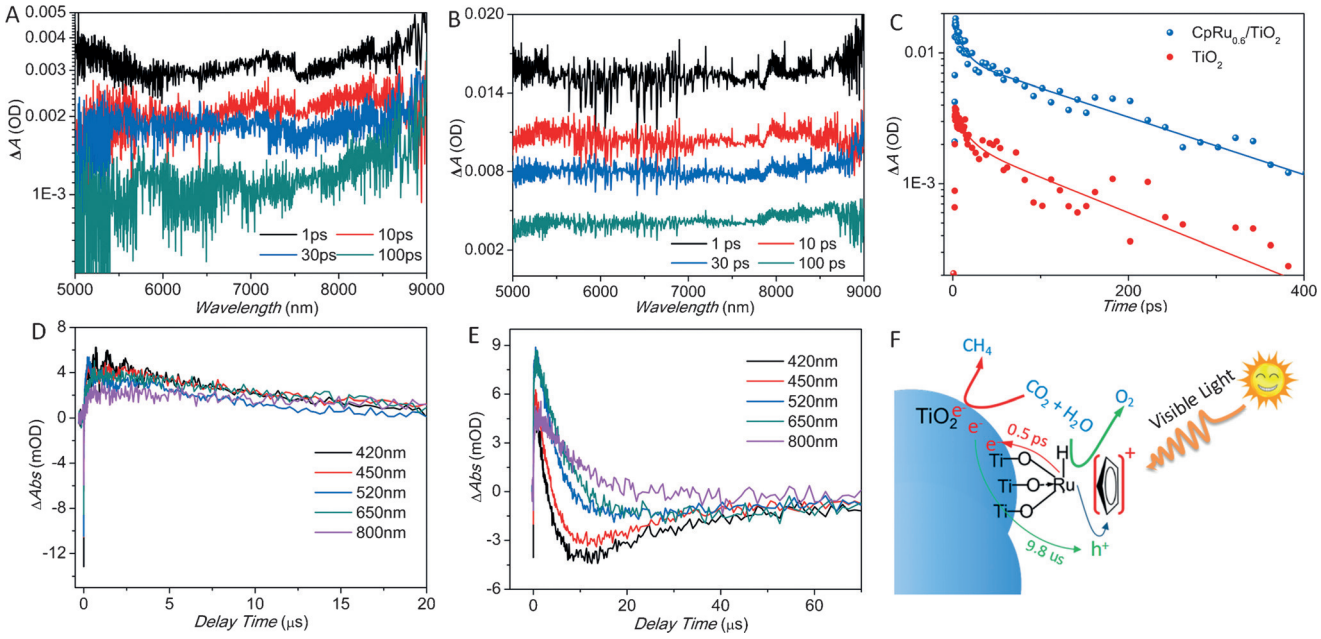

Figure 3. 800 nm laser excitation femtosecond time-resolved IR absorption spectra of TiO_2 (A) and $CpRu_{0.6}/TiO_2$ (B). C) Electron decay kinetics at 8500 nm. Fit curves are shown by solid line. The 355 nm laser excitation nanosecond absorption kinetics traces at different wavelengths of TiO_2 (D) and $CpRu_{0.6}/TiO_2$ (E). F) The proposed mechanism of photo-induced charge transfer in C_5H_5-RuH-TiO_2.

decay kinetics can be fitted by a biexponential decay process. The fit results of bare TiO_2 (Table S4) shows that the lifetime of fast component, attributable to trapping of electrons at shallow mid-gap states of TiO_2 nanoparticles, is 9.3 ± 3.1 ps, and the lifetime of slow component, belonging to bulk trapping process and charge recombination of electrons in TiO_2, is 142.0 ± 20.9 ps.[14] For the $CpRu_{0.6}/TiO_2$, the lifetime of the fast decay component is 7.0 ± 1.0 ps, which is basically the same as that of the bare TiO_2 when error is considered. Therefore, this fast component is assigned to the same process as that in bare TiO_2. Accordingly, the slow component with a lifetime of 186.0 ± 14.5 ps can be assigned to relaxation into deep bulk trapping sites and the back electron transfer into the surface C_5H_5-Ru complex. The relaxation time of photogenerated electrons is increased by ca. 43.5 ps in magnitude. It is thus expected that a long-lived charge-separated state of surface Ru complex can be formed after excitation with visible light, which is favorable for the interfacial transfer of electrons to reactive substrates.

To further explore the nature of the solar-fuel production, we applied nanosecond transient absorption (NTA) spectroscopy to follow the carrier dynamics in bare TiO_2 and $CpRu_{0.6}/TiO_2$ films under 355 nm light excitation. Figure 3 D,E display the decay kinetics of bare TiO_2 and $CpRu_{0.6}/TiO_2$ at different wavelength absorptions. For the bare TiO_2 (Figure 3 D), The kinetic traces exhibit a significant photo-bleaching or excited-state quenching on several nanosecond delay time scale, following by the formation and decay of charge-separated states at microsecond delay time. They could be fitted by a tri-exponential function. The fit results display that the NTA signatures at 420, 450, 520, 650, and 800 nm, respectively, representing holes trapped on surface, subsurface, and bulk centers as well as electrons trapped surface and subsurface centers, include one exciton formation process on the nanosecond time scale, one charge separation process and one charge recombination process on the microsecond time scale. Analysis of the quenching kinetics reveals that the exciton formation time is relatively constant, varying between 2.0 and 5.0 ns (Table S5). The charge-trapped species at 800 nm exhibits an electron transit time of 145.0 ± 2.0 ns and a recombination lifetime of 25.9 ± 4.0 μs. However, the kinetic traces of $CpRu_{0.6}/TiO_2$ become complex (Figure 3 E). Analysis of the kinetic traces by a bi-exponential function reveals clearly that the charge-separated state at 800 nm has a slight slower charge-separation lifetime of 185.9 ± 25.7 ns, and a charge-recombination lifetime of 9.8 ± 0.80 μs nearly three-fold faster than that of bare TiO_2 (Table S6). Therefore, we can sure that the NTA spectra are mainly contributed from the grafted C_5H_5-RuH complex. It is reasonable to propose that the charge transfer mechanism depicted in Figure 3 F occurs on the surface C_5H_5-RuH complex. The formation of the long-lived D^+–C–A^- charge-separated state, $C_5H_5^+$-RuH-O-TiO_2^-, is the key to the efficiently photocatalyzed fuel production in the artificial photosystem.

In summary, a new "push–pull" DCA triad as a photocatalyst has been successfully designed to mimic natural photosystems for CO_2 reduction based on both of the local surface excitation and the well-matched redox potentials. Such a hybrid material features the mononuclear C_5H_5-RuH surface complex binding to three Ti-O sites, in which the C_5H_5 ligand, the Ru^{2+} cation, and the TiO_2 moiety serve, respectively, as electron donor, light-harvester, and water-oxidation center, as well as electron acceptor and CO_2-reduction site. On irradiation, the hybrid forms a long-lived charge-separated state to carry out the CO_2-to-CH_4 conversion, showing an excellent photoactivity. A quantum efficiency of 0.56 %

can be achieved under visible light irradiation. This work provides visible opportunities for exploring at a molecular level the CO_2 photoreduction mechanism by design of a structurally well-defined photoactive center.

Acknowledgements

This work was financially supported by the NSFC (Grants Nos. 21373051 and U1305242), National Key Technologies R&D Program of China (2014BAC13B03), and 973 program (2013CB834800), We are grateful for Professor Lirong Zheng (BSRF), Professor Yuying Huang, and Professor Jinyuan Ma (SSRF) for the XAFS experiments.

Keywords: anatase · ruthenium complexes · charge-separated state · CO_2 reduction · photocatalysis

How to cite: *Angew. Chem. Int. Ed.* **2016**, *55*, 8314–8318
Angew. Chem. **2016**, *128*, 8454–8458

[1] T. Sakakura, J. C. Choi, H. Yasuda, *Chem. Rev.* **2007**, *107*, 2365–2387.
[2] a) Y. Izumi, *Coord. Chem. Rev.* **2013**, *257*, 171–186; b) S. C. Roy, O. K. Varghese, M. Paulose, C. A. Grimes, *ACS Nano* **2010**, *4*, 1259–1278; c) B. Kumar, M. Llorente, J. Froehlich, T. Dang, A. Sathrum, C. P. Kubiak, *Annu. Rev. Phys. Chem.* **2012**, *63*, 541–569; d) W. Tu, Y. Zhou, Z. Zou, *Adv. Mater.* **2014**, *26*, 4607–4626; e) A. J. Morris, G. J. Meyer, E. Fujita, *Acc. Chem. Res.* **2009**, *42*, 1983–1994; f) T. Zhang, W. Lin, *Chem. Soc. Rev.* **2014**, *43*, 5982–5993.
[3] S. N. Habisreutinger, L. Schmidt-Mende, J. K. Stolarczyk, *Angew. Chem. Int. Ed.* **2013**, *52*, 7372–7408; *Angew. Chem.* **2013**, *125*, 7516–7557.
[4] Y. Ma, X. Wang, Y. Jia, X. Chen, H. Han, C. Li, *Chem. Rev.* **2014**, *114*, 9987–10043.
[5] a) J. C. Swarts, A. Nafady, J. H. Roudebush, S. Trupia, W. E. Geiger, *Inorg. Chem.* **2009**, *48*, 2156–2165; b) L. Fan, J. Long, Q. Gu, H. Huang, H. Lin, X. Wang, *J. Catal.* **2014**, *320*, 147–159; c) J. Long, X. Wang, G. Zhang, J. Dong, T. Yan, Z. Li, X. Fu, *Chem. Eur. J.* **2007**, *13*, 7890–7899.
[6] a) J. H. Choi, L. E. Heim, M. Ahrens, M. H. Prechtl, *Dalton Trans.* **2014**, *43*, 17248–17254; b) O. Kozachuk, I. Luz, F. X. Llabrés i Xamena, H. Noei, M. Kauer, H. B. Albada, E. D. Bloch, B. Marler, Y. Wang, M. Muhler, *Angew. Chem. Int. Ed.* **2014**, *53*, 7058–7062; *Angew. Chem.* **2014**, *126*, 7178–7182.
[7] S. Ogo, R. Kabe, H. Hayashi, R. Harada, S. Fukuzumi, *Dalton Trans.* **2006**, 4657–4663.
[8] a) M. Zynek, M. Serantoni, S. Beloshapkin, E. Dempsey, T. McCormac, *Electroanalysis* **2007**, *19*, 681–689; b) P. G. Gassman, C. H. Winter, *J. Am. Chem. Soc.* **1988**, *110*, 6130–6135.
[9] a) D. Behar, H. Frei, M. Macnaughtan, J. Rabani, *J. Phys. Chem. C* **2012**, *116*, 23477–23484; b) R. Nakamura, A. Okamoto, H. Osawa, H. Frie, K. Hashimoto, *J. Am. Chem. Soc.* **2007**, *129*, 9596–9597.
[10] a) Q. Gu, J. Long, L. Fan, L. Chen, L. Zhao, H. Lin, X. Wang, *J. Catal.* **2013**, *303*, 141–155; b) M. T. Uddin, Y. Nicolas, C. Olivier, T. Toupance, M. M. Müller, H. J. Kleebe, K. Rachut, J. Ziegler, A. Klein, W. Jaegermann, *J. Phys. Chem. C* **2013**, *117*, 22098–22110.
[11] a) K. Iwata, T. Takaya, H. O. Hamaguchi, A. Yamakata, T. A. Ishibashi, H. Onishi, H. Kuroda, *J. Phys. Chem. B* **2004**, *108*, 20233–20239; b) A. Yamakata, T. Ishibashi, H. Onishi, *Chem. Phys. Lett.* **2001**, *333*, 271–277.
[12] a) G. Kobbe, C. Klingshirn, *Z. Phys. B* **1980**, *37*, 9–12; b) M. Trejo-Valdez, R. Torres-Martinez, N. Perea-Lopez, P. Santiago-Jacinto, C. Torres-Torres, *J. Phys. Chem. C* **2010**, *114*, 10108–10113; c) D. Torres-Torres, M. Trejo-Valdez, L. Castañeda, C. Torres-Torres, L. Tamayo-Rivera, R. C. Fernández-Hernández, J. A. Reyes-Esqueda, J. Muñoz-Saldaña, R. Rangel-Rojo, A. Oliver, *Opt. Express* **2010**, *18*, 16406–16417.
[13] A. Yamakata, T. Ishibashi, H. Onishi, *J. Phys. Chem. B* **2001**, *105*, 7258–7262.
[14] Y. Tamaki, K. Hara, R. Katoh, M. Tachiya, A. Furube, *J. Phys. Chem. C* **2009**, *113*, 11741–11746.

Received: March 20, 2016
Revised: April 23, 2016
Published online: May 30, 2016

